

Facile Fabrication of Anodic Alumina Rod-Capped Nanopore Films with Condensate Microdrop Self-Propelling Function

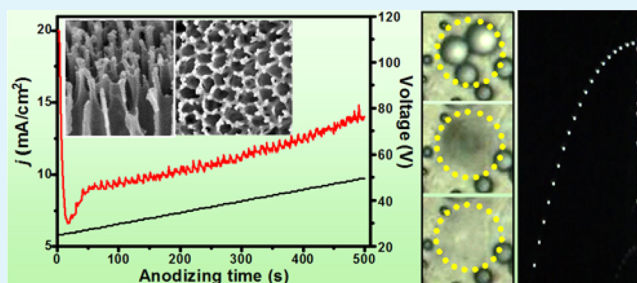
Juan Li,[†] Wenjing Zhang,[†] Yuting Luo, Jie Zhu, and Xuefeng Gao^{*}

Division of Nanobionic Research, Suzhou Institute of Nano-Tech and Nano-Bionics, Chinese Academy of Sciences, Suzhou 215123, P. R. China

Supporting Information

ABSTRACT: We report that aluminum surfaces can be endowed with condensate microdrop self-propelling (CMDSP) function by one-step voltage-rising mild anodization in hot phosphoric acid solution followed by fluorosilane modification. Via regulating reaction parameters, we can achieve anodic alumina self-standing rod-capped nanopore films and minimize their solid–liquid interface adhesion. Such low-adhesive nanostructured film owns remarkable CMDSP function, especially to condensate microdrops with sizes below 50 μm , differing from usual gravity-driven dropwise condensation on flat aluminum surfaces. Clearly, this work offers a facile, efficient, and industry-compatible approach to processing CMDSP aluminum materials, which is significant for developing innovative energy-saving air-conditioner heat exchangers.

KEYWORDS: low-adhesive, alumina rod-capped nanopores, condensate microdrop self-propelling, anodization, etching



Condensate microdrop self-propelling (CMDSP) surfaces^{1–23} have attracted intensive interest because of their value in basic research and technological innovations such as moisture self-cleaning,¹⁴ antifrosting,^{15–18} and enhancing condensation heat transfer for higher efficiency of thermal management and energy utilization.^{19–22} Differing from the gravity-driven shedding mode of condensate on usual hydrophobic flat surfaces, such CMDSP surface can realize the efficient self-jumping of small-scale condensate microdrops via their coalescence-released excess surface energy, without requiring external forces such as gravity and steam shear force.²³ It has been reported that the CMDSP surfaces not only own excellent antifrosting ability^{15–18} but can sustain frost-free by aiding with energy-effective intermittent weak airflow heating,¹⁸ which offers an innovative approach to developing more energy-saving air-conditioners and heat pumps. However, it is still a great challenge to find a facile, efficient, and industry-compatible approach to endowing engineering aluminum materials with desired CMDSP function. Recently, He et al. have reported that aluminum surfaces can be endowed with CMDSP function via hot water immersion followed by fluorosilane modification.^{8,9} However, the formed porous nanostructure, made of poorly crystallized aluminum hydroxide, is intrinsically unstable from either the chemical or mechanical perspective and thus is almost impossible to be used in practical applications.²⁴ It is well-known that electrochemical anodization is a type of widely used technologies for improving the surface properties of engineering aluminum materials such as hardening and anticorrosion.²⁵ However, usual anodic alumina nanopores cannot induce the desired CMDSP function because

of their strong solid–liquid interface adhesion (Figure S1). Very recently, we demonstrated that anodic alumina films consisting of self-standing rod-capped nanopores with extremely low solid–liquid interface adhesion may be used as ideal CMDSP aluminum surface.¹⁰ However, the developed nanofabrication technology requires multistep anodization and chemical etching, which is very tedious and time-consuming.

The current issue is how to establish a new type of one-step electrochemical anodization technology that can realize the rapid fabrication of alumina self-standing rod-capped nanopores. In principle, to achieve anodic alumina self-standing rod-capped nanopores, the utilization of etching effect is indispensable since pure anodization effects can only form hexagonally packed cells made of alumina nanopores with interconnecting solid walls.¹⁰ It is known that phosphoric acid (H_3PO_4) can be used as either the electrolyte for anodizing aluminum surfaces to form cylindrical alumina nanopores or the etchant for thinning alumina nanopore walls. Usually, these two utilities of H_3PO_4 have been separately used in previous studies and their used temperature ranges are different, e.g., 0 °C as the electrolyte²⁶ and ~ 30 °C as the etchant.²⁷ Besides, the growth rate of alumina nanopores can apparently increase with the increase of current density, which can be regulated by anodizing voltage, and the etching rate of alumina can be enhanced in the heated phosphoric acid solution. Based on these basic principles, we suppose that alumina self-standing

Received: June 23, 2015

Accepted: August 13, 2015

Published: August 13, 2015

rod-capped nanopores can rapidly form on aluminum surfaces by one-step voltage-rising mild anodization in hot H_3PO_4 solution. With the reaction proceeding, the growth rate of alumina nanopores can gradually accelerate so that previously formed relatively shorter segments near the top layer may experience opportune etching to form separated self-standing nanorods at the junction points of alumina cells, whereas later-formed relatively longer segments may keep their skeleton almost intact due to their insufficient etching. Accordingly, via synergistic control over the electrochemical parameters such as reaction time, temperature, H_3PO_4 concentration and initial voltage, we can rapidly obtain alumina self-standing rod-capped nanopore films with extremely low solid–liquid contact area and interface adhesion, which is the key to develop CMDSP aluminum materials.

Here, we have demonstrated that aluminum surfaces can be endowed with desired CMDSP function by one-step voltage-rising mild anodization in hot phosphoric acid solution followed by fluorosilane modification. Via optimizing reaction parameters, we can achieve the self-standing alumina rod-capped nanopores with minimized solid–liquid adhesion. Subsequent condensation experiments indicate that such low-adhesive nanostructure owns remarkable CMDSP function. Differing from the gravity-driven dropwise condensation on flat aluminum surfaces, small-scale condensate microdrops, especially those with sizes below $50\ \mu\text{m}$, can effectively self-remove on the nanosample surface via their coalescence-released excess surface energy.

Figure 1a shows the scanning electronic microscopic (SEM) top-view and side-view of the as-prepared self-standing alumina rod-capped nanopore sample. Typically, they can be achieved by anodizing aluminum foils in 2 vol % aqueous H_3PO_4 solution at $50\ ^\circ\text{C}$ for 500 s in one-step voltage-rising way, where the set anodization voltage increases linearly from the initial 25 V at the rate of 0.5 V per 10 s. Evidently, alumina rod-capped nanopores can uniformly cover the aluminum surface. From their SEM top-views, we can measure the average diameter ($\sim 120\ \text{nm}$) and period ($\sim 160\ \text{nm}$) of nanopores, respectively. From the SEM side-views, we know that the total film thickness is $1.5\ \mu\text{m}$, which includes contributions from both top-layer self-standing nanorods and bottom-layer nanopores. From the magnified side-view as shown in the inset of Figure 1a, we can know that the average diameter and height of the self-standing nanorods are 25 and 350 nm, respectively. Besides, we real-time monitor the variation of current densities (j) during the anodization process, as shown in Figure 1b. We found that with the anodization voltage increasing linearly, the j value first dramatically decreases from ~ 20 down to $\sim 6.5\ \text{mA}/\text{cm}^2$ (corresponding to the formation of barrier layer), then fast increases to $\sim 9\ \text{mA}/\text{cm}^2$ (corresponding to the initiation of pores) and afterward gradually increase up to $14.5\ \text{mA}/\text{cm}^2$ (corresponding to the formation of rod-capped pores).²⁸ Clearly, our method has typical advantages of operation simplicity (only requiring one-step reaction), rapid fabrication (only taking 500 s) and reaction mildness (the applied maximal current density less than $14.5\ \text{mA}/\text{cm}^2$).

In principle, the lower the solid–liquid interface adhesion, the smaller the dissipation of coalescence-released surface energy, which means that more energy can be used for driving the self-jumping of merged drops.²³ Clearly, it is very crucial to optimize electrochemical parameters such as reaction time (t), temperature (T), H_3PO_4 concentration (C), and anodizing voltage to achieve alumina self-standing rod-capped nanopores

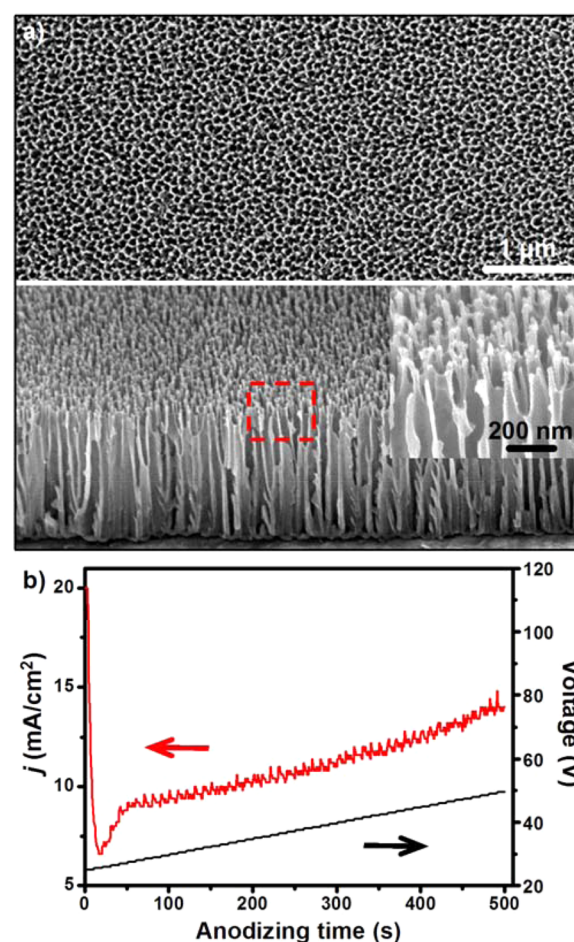


Figure 1. (a) Typical SEM top-view (top) and side-view (bottom) of alumina self-standing rod-capped nanopores covered on the aluminum surface. Magnified side-view of nanorods is shown as the inset. (b) Recorded current densities (j) varied with time during one-step voltage-rising anodization process.

with the minimized solid–liquid interface adhesion (F). To simplify experiments and, crucially, ensure relatively mild reaction condition, we performed all anodization reactions under the exemplified anodizing voltages that linearly increase from the initial 25 V at the rate of 0.5 V per 10 s. All data are summarized in Table 1 and the corresponding SEM images are shown in Figure S2. First, we study the effects of reaction time and found that alumina self-standing rod-capped nanopores

Table 1. Influence of Reaction Parameters to the Solid–Liquid Interface Adhesion of Anodized Aluminum Surfaces^a

sample	t (s)	T ($^\circ\text{C}$)	C (wt%)	F (μN)	etching degree
a1	100	50	2	69 ± 8	insufficient etching
a2	300	50	2	32 ± 5	insufficient etching
a3	500	50	2	0	rod-capped nanopore
b1	500	30	2	76 ± 4	insufficient etching
b2	500	40	2	55 ± 3	insufficient etching
b3	500	50	2	0	rod-capped nanopore
c1	500	50	1	8 ± 1	insufficient etching
c2	500	50	2	0	rod-capped nanopore
c3	500	50	4	0	over etching

^aHere, t , T , C , and F denote reaction time, temperature, H_3PO_4 concentration, and adhesive force, respectively.

with minimal interface adhesion (Figure S3) can be achieved as $t = 500$ s while fixing $T = 50$ °C and $C = 2$ vol %. As for relatively shorter reaction, anodized aluminum surfaces are still adhesive to the tested water droplets due to the insufficient etching of top-layer nanopores. For example, as $t = 100$ s, only nanopores with the film thickness of ~ 260 nm can form and the F value of the nanostructured surface is 69 μN ; as $t = 300$ s, the film thickness reaches ~ 830 nm and rodlike protuberances partially emerge on the top of nanopores, resulting in a lower F value (32 μN). Second, we further explore the influence of T in the case of $t = 500$ s and $C = 2$ vol %, and found that the self-standing rod-capped nanopores with minimal F value can form as $T = 50$ °C. In sharp contrast, for lower reaction temperatures, the anodized aluminum surfaces are adhesive (e.g., 76 μN for 30 °C samples and 55 μN for 40 °C samples) because of insufficient etching of top-layer nanopores. Third, we found that a proper H_3PO_4 concentration ($C = 2$ vol %) is also very crucial in the case of $t = 500$ s and $T = 50$ °C. As for lower concentration (e.g., $C = 1$ vol %), the formed nanorods standing on nanopores appear relatively blunter and thus present slight adhesion (8 μN). Note that the adhesive force of anodized aluminum surfaces may also become nonsticky to tested water droplets as $C = 4$ vol % but the formed nanorods bundle together, which is undesired.¹⁰ Therefore, the self-standing rod-capped nanopores with minimal interface adhesion can be achieved via controlling proper reaction parameters.

Subsequent condensation experiments indicate that such low-adhesive nanostructure indeed has the desired CMDSP function. All experiments are carried out under the identical condition with substrate temperature of ~ 1 °C, ambient temperature of ~ 25 °C and relative humidity of $\sim 80\%$ (for details, see Experimental Section in Supporting Information). Figure 2a shows the typical optical top-views of self-departure instant of condensate microdrops on the horizontal nanosample surface. Evidently, in-plane coalescence of adjacent condensate microdrops, caused by their individual condensation growth, can trigger the out-of-plane jumping of merged drops. Interestingly, it is easily found in the experiments that, as

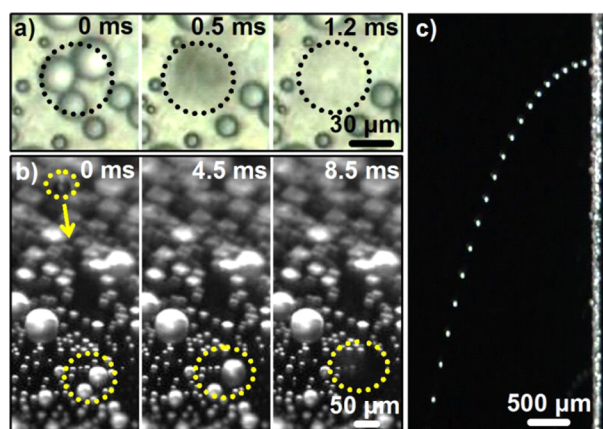


Figure 2. (a) Time-lapse optical top-views showing that condensate microdrops on the horizontal nanosample surface can instantly self-depart via their mutual coalescence. (b) Time-lapse optical tilted-views showing that a falling drop can impact the quasi-static condensate microdrops on the horizontal nanosample surface and initiate their self-jumping. (c) Overlapped optical side-view showing the trajectory of a merged microdrop ejecting from the vertical nanosample.

for horizontally placed nanosamples, the ejected microdrops can fall back to their surface and trigger new dynamical impact-induced self-propelling events (Figure 2b). Remarkably, the self-propelled jumping behaviors of microdrops are independent to the sample orientation. As shown in Figure 2c, merged condensate microdrops can eject from the vertical nanosample surface and fall along a parabolic trajectory. Note that the self-propelled jumping of condensate microdrops is universal and violent on the whole nanosample surface.

To more intuitively exhibit the advantage of our as-prepared nanostructured aluminum surfaces in controlling the self-removal of condensate drops at micrometer scale, we further explore their long-term dynamic condensation behaviors. Figure 3a shows the typical time-lapse optical top-views of

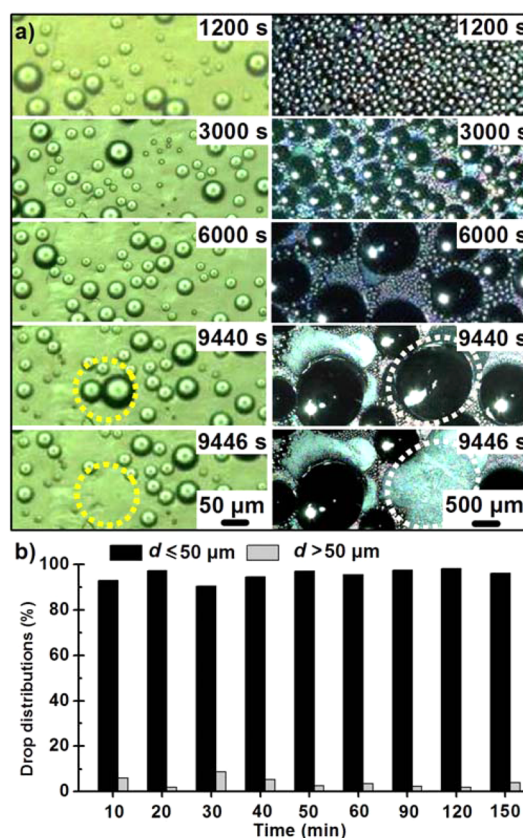


Figure 3. (a) Time-lapse optical top-views showing the long-term condensation behaviors of the vertical nanosample (left panel) and contrast flat aluminum sample (right panel). Compared with gravity-driven sliding of millimeter-scale condensate drops on the flat surface, small-scale condensate microdrops on the nanostructured surface can continuously self-remove in the jumping mode. (b) Drop number distribution of condensate microdrops with diameters (d) of ≤ 50 μm and > 50 μm varied with time.

condensate drop evolution of the nanostructured (left panel) and flat (right panel) aluminum surfaces. Evidently, as for the nanostructured surface, the sizes of condensate drops always maintain at micrometer scale and these tiny drops can dynamically self-depart. In sharp contrast, condensate drops on the flat aluminum surface can merge but cannot timely self-depart due to their strong solid–liquid interface adhesion. As a result, these growing drops can long-term reside on the flat surface and only slide off under gravity until their sizes reaching millimeter scale. To quantify and highlight the CMDSP

performance of our nanosamples at the microscale, we further analyze drop number distribution of residence microdrops with diameters (d) $\leq 50 \mu\text{m}$ and $>50 \mu\text{m}$, as shown in Figure 3b. Remarkably, condensate microdrops with $d \leq 50 \mu\text{m}$ dominate on the nanosample surface and present a slight fluctuation with the time extending while microdrops with $d > 50 \mu\text{m}$ occupy less than 10%. Compared with the flat aluminum surface, our as-prepared nanosample can efficiently control the sizes of residence condensate drops at micrometer scale, especially below $50 \mu\text{m}$. In other words, these small-scale condensate microdrops can effectively self-remove on the nanosample surface.

In conclusion, we have demonstrated that aluminum surfaces can be endowed with CMDSP function by one-step voltage-rising mild anodization in hot phosphoric acid solution followed by fluorosilane modification. This method is very facile, efficient, cheap, industry-compatible and promising to be developed into practical aluminum-based surface nanoengineering technologies. Clearly, this work offers a new and more efficient avenue for developing CMDSP Al materials, which are significant to develop innovative more energy-saving air-conditioners and heat pumps. Currently, our group is using such nanofabrication technology to develop practical CMDSP air-conditioner Al fins and evaluate their antideicing and antifrosting utilities and consequently energy-saving effects. In addition, such CMDSP Al surface owns perfect nonstickiness to the impinging macroscopic water droplets (Figure S4), which can also find important applications such as raindrop self-cleaning, fluid drag-reducing, and subcooled water antifreezing.

■ ASSOCIATED CONTENT

Supporting Information

The Supporting Information is available free of charge on the ACS Publications website at DOI: 10.1021/acsami.5b05564.

Experimental details and additional data, including the condensation behavior of usual nanopore structured surface (Figure S1), SEM top-views and side-views of alumina nanopore structures as-achieved under different reaction conditions (Figure S2), adhesive force curves of the optimal rod-capped nanopore structure surface and flat surface (Figure S3), and perfect nonstickiness of the nanosample surface to an impinging macroscopic water droplet (Figure S4) (PDF)

■ AUTHOR INFORMATION

Corresponding Author

*E-mail: xfgao2007@sinano.ac.cn.

Author Contributions

[†]J.L. and W.Z. contributed equally.

Notes

The authors declare no competing financial interest.

■ ACKNOWLEDGMENTS

This work was supported by the National Basic Research Program of China (2012CB933200), Key Research Program of the Chinese Academy of Sciences (KJZD-EW-M01), National Natural Science Foundation of China (201403285), Natural Science Foundation of Jiangsu Province (BK20130355), China Postdoctoral Science Foundation (2013M541746), and Suzhou Institute of Nano-Tech and Nano-Bionics, CAS.

■ REFERENCES

- (1) Chen, C.-H.; Cai, Q.; Tsai, C.; Chen, C.-L.; Xiong, G.; Yu, Y.; Ren, I. Dropwise Condensation on Superhydrophobic Surfaces with Two-Tier Roughness. *Appl. Phys. Lett.* **2007**, *90*, 173108.
- (2) Boreyko, J. B.; Chen, C.-H. Self-Propelled Dropwise Condensate on Superhydrophobic Surfaces. *Phys. Rev. Lett.* **2009**, *103*, 184501.
- (3) Chen, X.; Wu, J.; Ma, R.; Hua, M.; Koratkar, N.; Yao, S.; Wang, Z. Nanograsped Micropylamidal Architectures for Continuous Dropwise Condensation. *Adv. Funct. Mater.* **2011**, *21*, 4617–4623.
- (4) Boreyko, J. B.; Zhao, Y. J.; Chen, C.-H. Planar Jumping-Drop Thermal Diodes. *Appl. Phys. Lett.* **2011**, *99*, 234105.
- (5) Feng, J.; Qin, Z.; Yao, S. Factors Affecting the Spontaneous Motion of Condensate Drops on Superhydrophobic Copper Surfaces. *Langmuir* **2012**, *28*, 6067–6075.
- (6) Feng, J.; Pang, Y.; Qin, Z.; Ma, R.; Yao, S. Why Condensate Drops Can Spontaneously Move Away on Some Superhydrophobic Surfaces but Not on Others. *ACS Appl. Mater. Interfaces* **2012**, *4*, 6618–6625.
- (7) Luo, Y.; Li, J.; Zhu, J.; Zhao, Y.; Gao, X. Fabrication of Condensate Microdrop Self-Propelling Porous Films of Cerium Oxide Nanoparticles on Copper Surfaces. *Angew. Chem., Int. Ed.* **2015**, *54*, 4876–4879.
- (8) He, M.; Zhou, X.; Zeng, X.; Cui, D.; Zhang, Q.; Chen, J.; Li, H.; Wang, J.; Cao, Z.; Song, Y.; Jiang, L. Hierarchically Structured Porous Aluminum Surfaces for High-Efficient Removal of Condensed Water. *Soft Matter* **2012**, *8*, 6680–6683.
- (9) He, M.; Zhang, Q.; Zeng, X.; Cui, D.; Chen, J.; Li, H.; Wang, J.; Song, Y. Hierarchical Porous Surface for Efficiently Controlling Microdroplets' Self-Removal. *Adv. Mater.* **2013**, *25*, 2291–2295.
- (10) Zhao, Y.; Luo, Y.; Li, J.; Yin, F.; Zhu, J.; Gao, X. Condensate Microdrop Self-Propelling Aluminum Surfaces Based on Controllable Fabrication of Alumina Rod-Capped Nanopores. *ACS Appl. Mater. Interfaces* **2015**, *7*, 11079–11082.
- (11) Miljkovic, N.; Wang, E. N. Condensation Heat Transfer on Superhydrophobic Surfaces. *MRS Bull.* **2013**, *38*, 397–406.
- (12) Enright, R.; Miljkovic, N.; Alvarado, J. L.; Kim, K.; Rose, J. W. Dropwise Condensation on Micro and Nanostructured Surfaces. *Nanoscale Microscale Thermophys. Eng.* **2014**, *18*, 223–250.
- (13) Miljkovic, N.; Preston, D. J.; Enright, R.; Wang, E. N. Jumping-Droplet Electrostatic Energy Harvesting. *Appl. Phys. Lett.* **2014**, *105*, 013111.
- (14) Wisdom, K. M.; Watson, J. A.; Qu, X.; Liu, F.; Watson, G. S.; Chen, C.-H. Self-Cleaning of Superhydrophobic Surfaces by Self-Propelled Jumping Condensate. *Proc. Natl. Acad. Sci. U. S. A.* **2013**, *110*, 7992–7997.
- (15) Chen, X.; Ma, R.; Zhou, H.; Zhou, X.; Che, L.; Yao, S.; Wang, Z. Activating the Microscale Edge Effect in a Hierarchical Surface for Frosting Suppression and Defrosting Promotion. *Sci. Rep.* **2013**, *3*, 2515.
- (16) Boreyko, J. B.; Collier, C. P. Delayed Frost Growth on Jumping-Drop Superhydrophobic Surfaces. *ACS Nano* **2013**, *7*, 1618–1627.
- (17) Lv, J.; Song, Y.; Jiang, L.; Wang, J. Bio-Inspired Strategies for Anti-Icing. *ACS Nano* **2014**, *8*, 3152–3169.
- (18) Xu, Q.; Li, J.; Tian, J.; Zhu, J.; Gao, X. Energy-Effective Frost-Free Coatings Based on Superhydrophobic Aligned Nanocones. *ACS Appl. Mater. Interfaces* **2014**, *6*, 8976–8980.
- (19) Miljkovic, N.; Enright, R.; Nam, Y.; Lopez, K.; Dou, N.; Sack, J.; Wang, E. N. Jumping-Droplet-Enhanced Condensation on Scalable Superhydrophobic Nanostructured Surfaces. *Nano Lett.* **2013**, *13*, 179–187.
- (20) Hou, Y.; Yu, M.; Chen, X.; Wang, Z.; Yao, S. Recurrent Filmwise and Dropwise Condensation on a Beetle Mimetic Surface. *ACS Nano* **2015**, *9*, 71–81.
- (21) Zhu, J.; Luo, Y.; Tian, J.; Li, J.; Gao, X. Clustered Ribbed-Nanoneedle Structured Copper Surfaces with High-Efficiency Dropwise Condensation Heat Transfer Performance. *ACS Appl. Mater. Interfaces* **2015**, *7*, 10660–10665.
- (22) Zhao, Y.; Luo, Y.; Zhu, J.; Li, J.; Gao, X. Copper-Based Ultrathin Nickel Nanocone Films with High-Efficiency Dropwise Condensation

Heat Transfer Performance. *ACS Appl. Mater. Interfaces* **2015**, *7*, 11719–11723.

(23) Tian, J.; Zhu, J.; Guo, H.-Y.; Li, J.; Feng, X.-Q.; Gao, X. Efficient Self-Propelling of Small-Scale Condensed Microdrops by Closely-Packed ZnO Nanoneedles. *J. Phys. Chem. Lett.* **2014**, *5*, 2084–2088.

(24) Vedder, W.; Vermilyea, D. A. Aluminum + Water Reaction. *Trans. Faraday Soc.* **1969**, *65*, 561–584.

(25) Edward, G. *Corrosion Resistance of Aluminum and Magnesium Alloys: Understanding, Performance, and Testing*; Wiley-VCH: Weinheim, Germany, 2010; pp 477–511.

(26) Masuda, H.; Yada, K.; Osaka, A. Self-Ordering of Cell Configuration of Anodic Porous Alumina with Large-Size Pores in Phosphoric Acid Solution. *Jpn. J. Appl. Phys.* **1998**, *37*, 1340–1342.

(27) Li, J.; Li, C.; Chen, C.; Hao, Q.; Wang, Z.; Zhu, J.; Gao, X. Facile Method for Modulating the Profiles and Periods of Self-Ordered Three-Dimensional Alumina Taper-Nanopores. *ACS Appl. Mater. Interfaces* **2012**, *4*, 5678–5683.

(28) Li, J.; Li, C.; Gao, X. Structural Evolution of Self-Ordered Alumina Tapered Nanopores with 100 nm Interpore Distance. *Appl. Surf. Sci.* **2011**, *257*, 10390–10394.